Tropical Intra-Seasonal Oscillations in the DEMETER Multi-Model System

F. J. Doblas-Reyes, R. Hagedorn, T. Palmer and J.-Ph. Duvel*

ECMWF, Shinfield Park, RG2 9AX, Reading, UK
** LMD, CNRS, Ecole Normale Superieure, F-75230, Paris, France*

1. Abstract

An analysis of the features of the tropical intra-seasonal oscillations in the DEMETER multi-model dataset has been carried out. A range of different tropical intra-seasonal variability biases has been identified in the coupled models of the multi-model system, although those models sharing the same atmospheric component tend to present similar biases. These errors have been linked to systematic model errors such that the drawbacks in the simulation of the intra-seasonal oscillations in specific models may be traced back to problems in their atmospheric general circulation. Variability errors are not homogeneous in a wavenumber-frequency representation, so that the under or overestimation of the intra-seasonal variability may be due to drawbacks in the representation of particular oscillations, such as the Kelvin waves or the MJO. The analysis has shown that ocean-atmosphere coupling is a relevant element in the simulation of intra-seasonal oscillations, in particular of the MJO. However, it has been found that the choice of a particular ocean model does not seem to play a major role. Finally, a new strategy, based on the local mode analysis method, to estimate the seasonal predictability of the activity of intra-seasonal oscillations has been tested.

2. Introduction

Seasonal weather forecasts are of potential value for a wide cross section of society, for personal, commercial and humanitarian reasons. Dynamical seasonal forecasts have been made operationally using ensemble systems with perturbed initial conditions (Stockdale et al., 1998). However, if uncertainties in initial conditions were the only perturbations represented in a seasonal-forecast ensemble, then the resulting measures of predictability would not be reliable, the reason being that the model equations are also uncertain. One approach to this problem relies on the fact that global climate models have been developed somewhat independently at different climate research institutes. An ensemble comprising such quasi-independent models could therefore be thought of as providing a sampling of possible model equation sets. This is referred to as a multi-model ensemble (Palmer et al., 2000). A multi-model ensemble-based system for seasonal-to-interannual prediction has been developed in the European project DEMETER (Development of a European Multi-Model Ensemble Prediction System for Seasonal to Interannual Prediction). The DEMETER system comprises seven global atmosphere-ocean coupled models, and has been designed to study the multi-model concept by creating an extensive hindcast dataset. The comprehensive evaluation of this hindcast dataset demonstrates the enhanced reliability and skill of the multi-model ensemble over a more conventional single-model ensemble approach.

In addition to a technique to improve forecast quality, a multi-model system can also be considered as a unique tool to assess the ability of the prediction models to represent particular phenomena relevant to the forecasting process. Different models with similar overall forecast quality may agree to predict the correct climate anomaly of a specific event. This set of simulations would help to enlighten the mechanisms at the origin of the climate anomaly. On the other hand, the reasons to issue false alarms will differ among the models due to their distinct systematic errors. The systematic analysis and documentation of the model characteristics facilitates the understanding of the hits and false alarms and might, through the identification

of the physical processes involved, contribute to a potential improvement of the models. In theory, such analyses require that all models simulate the same time period under comparable experimental conditions, and that the same diagnostic measures of performance be calculated for all models. Therefore, the DEMETER hindcast dataset constitutes an ideal framework for this task. Among the whole set of phenomena to be used as a benchmark test for model performance, tropical intra-seasonal oscillations, which include propagating synoptic- and large-scale disturbances moving parallel to the equator, represent one of the most important targets of the climate modelling community (Slingo et al., 1996). More specifically, they bear some relationship with ENSO, the most important mode of variability in seasonal prediction, and are intimately linked to the model mean bias (Innes and Slingo, 2003).

3. Experiment and data

The DEMETER project1 has been funded under the European Union Vth Framework Environment Programme to assess the skill and potential economic value of multi-model ensemble seasonal forecasts. The principal aims of DEMETER have been to advance the concept of multi-model ensemble prediction by installing a number of state-of-the-art global coupled ocean-atmosphere models on a single supercomputer, to produce a series of multi-model ensemble hindcasts with common archiving and common diagnostic software, and to assess the utility of multi-model hindcasts in specific quantitative applications, notably health and agriculture.

The DEMETER multi-model prediction system comprises the global coupled ocean-atmosphere models of the following institutions: CERFACS (European Centre for Research and Advanced Training in Scientific Computation, France), ECMWF (European Centre for Medium-range Weather Forecasts), INGV (Istituto Nazionale de Geofisica e Vulcanologia, Italy), LODYC (Laboratoire d'Océanographie Dynamique et de Climatologie, France), MetFr (Météo-France, France), UKMO (Met Office, UK) and MPI (Max-Planck Institut für Meteorologie, Germany). In order to assess seasonal dependence on forecast skill, the DEMETER hindcasts have been started four times a year from 1st February, 1st May, 1st August, and 1st November at 00 GMT. The atmospheric and land-surface initial conditions are taken from the ECMWF Re-Analysis2 (ERA-40) dataset. The ocean initial conditions are obtained from ocean-only runs forced by ERA-40 fluxes, except in the case of MPI that used a coupled initialization method. Each hindcast has been integrated for 6 months and comprises an ensemble of 9 members. Hindcasts have been produced over the period 1958-2001, although the common period to all the models is 1980-2001. A large subset of atmosphere and ocean variables, both daily data and monthly means has been stored into the ECMWF's Meteorological Archival and Retrieval System (MARS). A significant part of the DEMETER dataset (monthly averages of a large subset of surface and upper-air fields) is now freely available for research purposes through a public online data retrieval system installed at ECMWF3. The data can be retrieved in both GRIB and NetCDF format.

The performance of the DEMETER system has been evaluated from this comprehensive set of hindcasts (Palmer et al., 2004). In addition, a complete set of diagnostics (performed in cross-validation mode) can be accessed on-line4. A key result is that multi-model ensemble probability scores are, on average, better than those from any of the single-model ensembles, this improvement not being only a consequence of the

[1] A complete description of the project and its main results can be found on the DEMETER website: http://www.ecmwf.int/research/demeter

[2] http://www.ecmwf.int/research/era

[3] Monthly data can be retrieved in GRIB and NetCDF from http://www.ecmwf.int/research/demeter/data

[4] http://www.ecmwf.int/research/demeter/verification

increase in ensemble size. Results indicate that the multi-model ensemble is a viable pragmatic approach to the problem of representing model uncertainty in seasonal-to-interannual prediction, leading to a more reliable and skilful forecasting system than that based on any one single model.

4. Intra-seasonal tropical variability

The single-model and multi-model ensembles in the DEMETER system have showed some useful skill in predicting seasonal climate anomalies (Palmer et al., 2004). This skill may be linked to characteristics of phenomena in the intra-seasonal frequency band. In order to test this hypothesis, the features of the intra-seasonal variability over the tropics have been assessed for several variables. First, the spatial distribution and strong seasonal cycle of the variability have been estimated. Secondly, a wavenumber-frequency spectral analysis has been carried out to discriminate between the different types of oscillations. Finally, an empirical orthogonal function (EOF) analysis has been used to estimate the main modes of variability. The results obtained with the ERA-40 dataset have been taken as reference. In the following, only the results from the hindcasts started in November (boreal winter) and May (boreal summer) for the period 1980-2001 will be discussed.

Figure 1 shows the intra-seasonal standard deviation of low-level zonal wind for ERA-40 and three of the coupled models in boreal winter (November to April) and summer (May to October). The standard deviation has been computed after removing the mean seasonal cycle and a linear trend estimated separately for each season and ensemble member. Variances for each ensemble member and hindcast have been calculated and then averaged to provide an unbiased estimate of the standard deviation comprising both the internal and external variability of the ensemble. While MetFr tends to overestimate the tropical variability, UKMO shows a clear underestimation. ECMWF displays a mixed behaviour, with a strong underestimation over the Indian Ocean in summer and a slight underestimation elsewhere. Similar results have been obtained for OLR as well as for other variables (200 and 850 hPa zonal wind). The overestimation in MetFr agrees well with an excess of mean westerly wind over the tropical western Pacific, not found for ECWMF and UKMO, and may be linked to a slightly higher skill of MetFr in the prediction of western tropical Pacific SSTs.

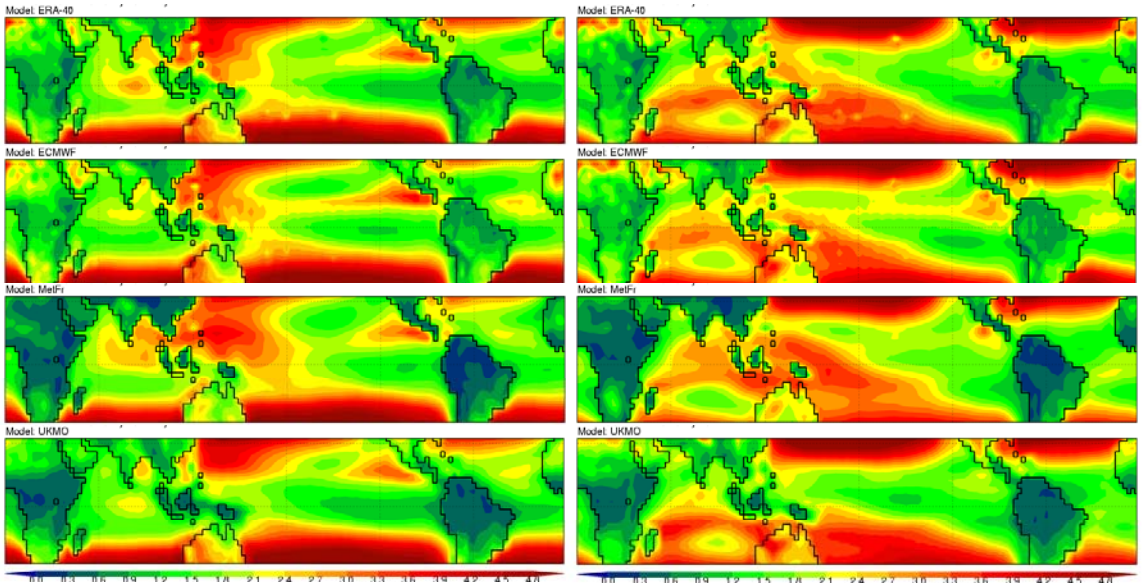

Figure 1: Intra-seasonal standard deviation of 10-metre zonal wind (in m/s) for ERA-40 (top row), ECMWF (second row), MetFr (third row) and UKMO (bottom row). The left column shows the results for boreal summer (May to October, hindcasts started in May) and the right one for boreal winter (November to April, hindcasts started in November).

The seasonal cycle of intra-seasonal variability can be observed in Figure 1. A southward shift of the maxima of tropical variability from north to south when changing from summer to winter can be noticed. This seasonal shift is found for every model, although the drawbacks of the intra-seasonal variability described above remain the same. It has been found that these errors in intra-seasonal variability are mainly dependent on the atmospheric component of the coupled model. Figure 2 displays the difference of standard deviation with respect to ERA-40 for the ECMWF (left) and LODYC (right) coupled models. These two models share the same atmospheric GCM (IFS), but use two different ocean models (HOPE and ORCA, respectively). The errors in intra-seasonal standard deviation have similar intensity and distribution. This result is not likely to be model dependent as similar results are obtained using another atmospheric GCM (ARPEGE) coupled to two different versions of an ocean GCM (not shown). However, this does not necessarily imply that coupling is not important. To illustrate the impact of ocean-atmosphere coupling, Figure 3 depicts the intra-seasonal standard deviation error for the UKMO experiment and for an additional set of hindcasts carried out with the same atmospheric component forced by persisted SSTs. Overall, the error is smaller in the coupled experiment, the reduction being more noticeable over the tropical Indian Ocean and northeastern tropical Pacific. The reduced variability bias of the coupled model when compared to the atmosphere-only experiment agrees well with the larger skill found for tropical precipitation (Palmer et al., 2004). The error reduction in intra-seasonal variability appears to be less important far from the surface, where the impact of coupling is smaller. The areas mentioned above are those where the impact of the coupling is stronger. The impact of the coupling can be considered as the local feedback carried out by surface fluxes, which has been estimated through the lagged correlation of SST and precipitation (not shown).

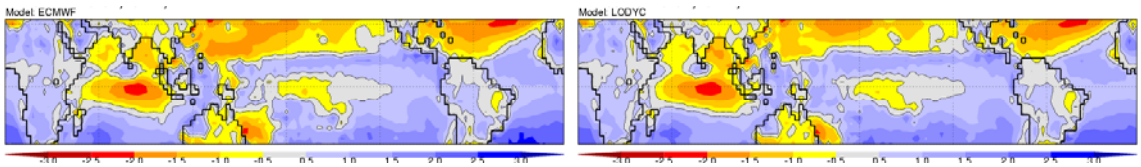

Figure 2: Difference of intra-seasonal standard deviation of 10-metre zonal wind (in m/s) with respect to ERA-40 of the ECMWF (left) and LODYC (right) hindcasts for boreal summer (May to October, hindcasts started in May). Yellow and red colours represent underestimation, while blue indicates overestimation.

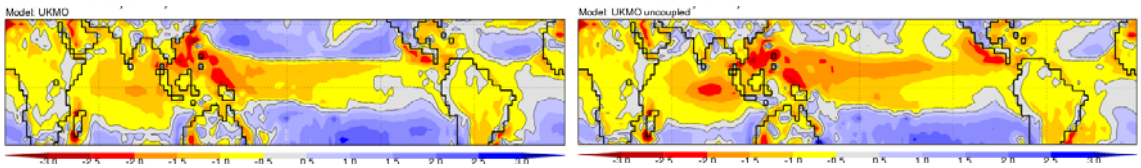

Figure 3: As Figure 2, but for the UKMO coupled (left) and uncoupled (right) hindcasts.

To discriminate between the different tropical intra-seasonal oscillations a space-time spectral analysis has been carried out (von Storch and Zwiers, 1999). This technique is useful for the study of zonally propagating waves as it decomposes the field dependent on time and longitude into wavenumber and frequency components for eastward and westward propagating waves. The approach described in Wheeler and Kiladis (1999) has been applied here. The mean seasonal cycle and an individual linear trend have been previously removed from each ensemble member and from the ERA-40 data as above. Then, a decomposition in symmetric and antisymmetric components around the equator has been carried out to take into account the different nature of linear equatorial waves. The zonal Fourier coefficients of the symmetric and antisymmetric components for each time step, latitude and ensemble member are computed. The wavenumber-frequency spectrum is then obtained by computing the spectrum of the zonal coefficients. The spectrum is then averaged over all available years and ensemble members (in the case of the hindcasts) and summed for the latitudes between 15ºN and 15ºS. Given the red nature of the raw spectra, a background

spectrum has been defined and removed from the original spectra to stand out the spectral peaks. The background spectrum is calculated as the average power of both the symmetric and antisymmetric spectra, smoothed many times in frequency and wavenumber with a low-pass filter. Finally, the individual spectra are divided by the background power.

Figure 4 shows the wavenumber-frequency spectrum of the symmetric component of boreal summer 10-metre zonal wind for ERA-40 and three coupled models. Spectra for temperature and wind for different levels in the troposphere are very similar, while the OLR spectrum depicts slightly different features. The signature of a number of oscillations can be identified. Signals of Kelvin waves are found in every model spectrum (frequency higher than 0.05 cpd and wavenumber larger than 1), although the dispersion curves are slightly different. For instance, MetFr tends to have faster Kelvin waves than any of the other models or ERA-40, while ECMWF and UKMO seem to underestimate their variance. Indications of mixed Rossby-gravity waves can be found at around 0.2 cpd for the range of westward planetary wavenumbers of 1 through 6. These oscillations appear in the spectrum of the antisymmetric component of OLR. They seem to be underestimated by MetFr and overestimated by UKMO. The equatorial Rossby waves (very low frequency, westward propagating wavenumbers from 1 to 4) have a reduced variance in the model's spectra. The appearance of the MJO is evidenced around 0.025 cpd for the range of eastward planetary wavenumbers of 1 through 3. To better illustrate the characteristics of these waves, Figure 5 displays a detailed view of the spectrum obtained with the four datasets for low-level zonal wind (left) and OLR (right). ERA-40 shows a broad peak for the range of 0.01 to 0.04 cpd and wavenumbers 1 through 3. This peak is very similar for both 10-metre wind and OLR. ECMWF and UKMO seem to underestimate the amplitude of the peak in 10-metre wind and have almost no signal in OLR, which can be better interpreted as a standing oscillation. MetFr is

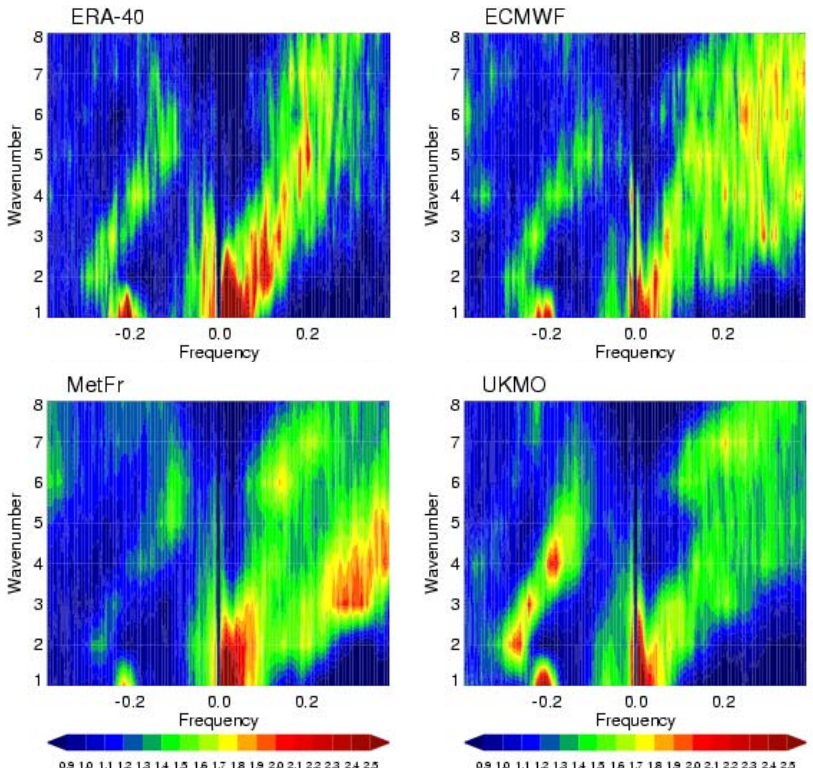

Figure 4: Wavenumber-frequency spectrum of the symmetric component of 10-metre zonal wind for ERA-40 (top left) and ECMWF (top right), MetFr (bottom left) and UKMO (bottom right) boreal summer hindcasts (May to October, hindcasts started in May). Positive (negative) frequencies in cpd correspond to eastward (westward) propagating waves.

the only model of the three presented here that shows a realistic (both in magnitude and spectral range) peak in 10-metre wind, but suffers from the same drawback as the other models for OLR. Winter spectra agree well with these results, except that a realistic peak is found this time for MetFr in OLR. These results suggest that the under or overestimation of the intra-seasonal variability are the result of drawbacks in specific intra-seasonal oscillations. In addition, among the models discussed here, MetFr seems to simulate intra-seasonal oscillations with the most realistic features, especially in the case of large-scale perturbations.

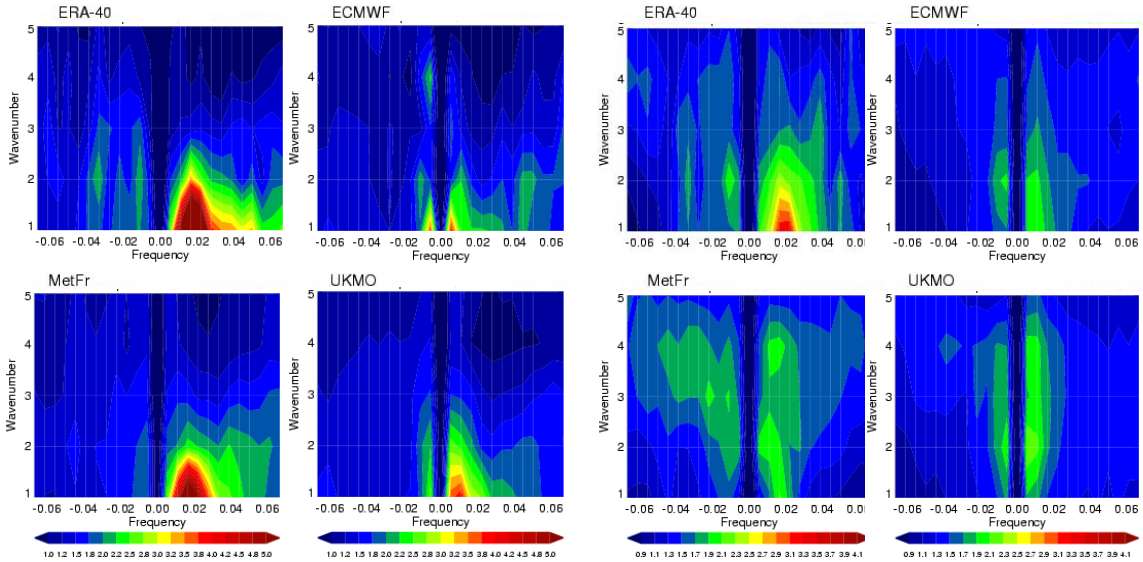

Figure 5: As in Figure 4, but for 10-metre zonal wind (left) and OLR (right). Note that the scale is different from that in Figure 4.

As another illustration of the benefits of ocean-atmosphere coupling, Figure 6 shows the wavenumber-frequency spectrum of the symmetric component of boreal summer 10-metre wind for the UKMO coupled and uncoupled experiments. The underestimation of the spectral power within the MJO band is smaller in the coupled experiment, indicating that coupling could make the simulated MJO more realistic, in agreement with the results of Inness and Slingo (2003).

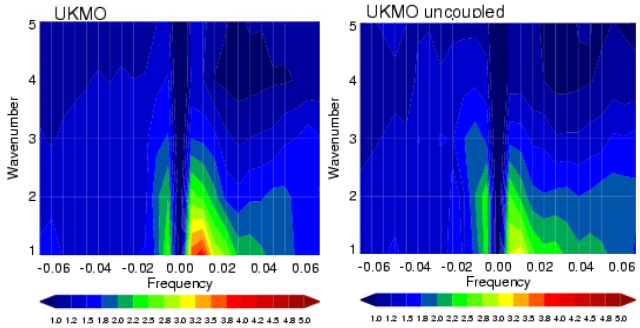

Figure 6: As in Figure 4, but for UKMO (left) and UKMO uncoupled (right). Note that the scale is different from that in Figure 4.

The previous spectral analysis indicates that the main drawbacks of the simulated intra-seasonal variability are found for the large-scale oscillations, which also generate most of the variability. Therefore, an EOF analysis has been used to estimate the characteristics of the main modes of intra-seasonal variability. The mean seasonal cycle has been previously removed. Then, a spectral filtering within the band 20-90 days has been applied to each time series. Figure 7 shows the two leading EOFs of the boreal summer 10-metre zonal wind for ERA-40 and three of the models. The percentage of variance explained by the first EOF is 11.3, 8.5, 10.5 and 8.2 for ERA-40, ECMWF, MetFr and UKMO, respectively. The percentage is 10.0, 7.1, 9.2 and 7.2

in the case of the second EOF. In all cases the variance is very similar between both EOFs, as in the case of a degenerated pair. The spatially shifted structures and the principal component lagged correlation that appear in ERA-40 and MetFr suggest that the pair of EOFs represent an eastward propagating planetary scale wave, which can be identified with the MJO. Some other well-identified structures appear also in the upper-level zonal wind, while the leading EOFs of the OLR show anomalies localized over the eastern Indian Ocean/western Pacific and Central America. The mode of variability represented by this pair of EOFs is particularly well simulated by MetFr, in agreement with the spectral description of the MJO shown in Figure 5. On the contrary, this pair is not well reproduced by UKMO while ECMWF misses the anomalies over the Indian Ocean in agreement with the systematic error of this model described above. It should be taken into account that some problems have been identified in the western branch of the Walker circulation, the low-level convergence over the Indo-Pacific area being spread over an excessively large area (not shown).

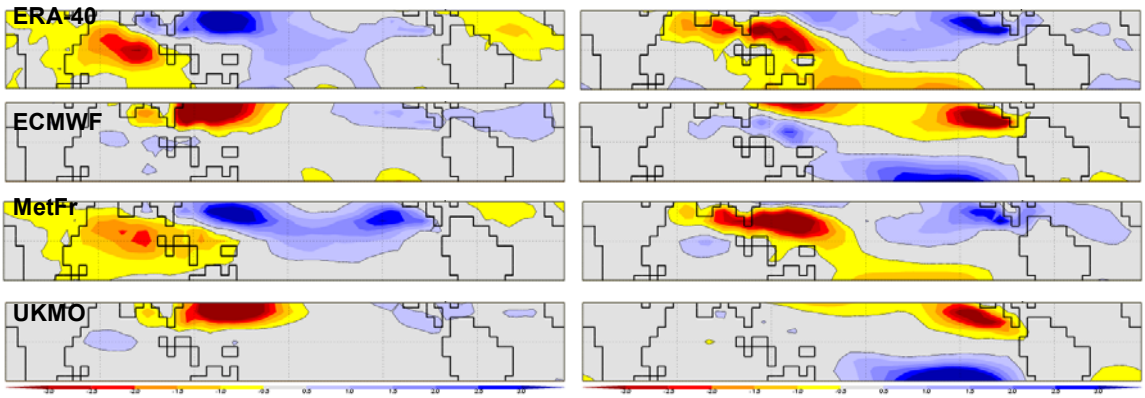

Figure 7: Leading EOFs (first EOF on the left, second on the right) of the 20-90 days filtered 10-metre wind for ERA-40 (top row) and ECMWF (second row), MetFr (third row) and UKMO (bottom row) boreal summer hindcasts (May to October, hindcasts started in May). Signs are arbitrary. Units are arbitrary for normalization purposes.

5. Inter-annual predictability of the intra-seasonal activity

Intra-seasonal variability displays substantial inter-annual variations in intensity. Although the reasons for this inter-annual variability are not yet understood (Slingo et al., 1999), the predictability of the seasonally averaged activity should be assessed given its link with the Austral-Asian monsoon and ENSO. The seasonal activity of the intra-seasonal variability has been estimated using the local mode analysis method (Goulet and Duvel, 2000). This method computes a complex principal component analysis over short time sections (90 days here) of the whole time series. The analysis is applied on a 5-day moving window, so that every five days a new analysis is done. Only the leading complex EOF mode from this analysis is retained. Retaining the leading complex component ensures that only the main mode of variability at every time interval is analysed, while the moving window approach with a short interval avoids a common drawback of all the analyses based on principal components i.e., the fact that the leading components correspond to average modes that may not be representative of intermittent perturbations. A time series of percentage of variance of each leading mode obtained every five days can be constructed, from which the local maxima are identified. The leading modes corresponding to these local maxima are called “local modes”. The spatial patterns of these local modes are more persistent in time and/or more spatially coherent than the patterns of other leading modes. Local mode analysis provides an estimate of the intra-seasonal signal time and space features and allows the detection of persistent and coherent (in a spatio-temporal sense) patterns that can be associated with physical perturbations. The method is particularly effective to characterize time-evolving large-scale intermittent oscillations. The computation has been carried out separately for each ensemble member in each hindcast.

Some preliminary results using boreal winter OLR are presented here. The region selected for the analysis is the tropical Indian Ocean (30ºN-20ºS and 40ºE-130ºE). The data have been spectrally filtered retaining the harmonics 1 to 6 (variability band of 15-90 days) within each 90-day window. To obtain local mode estimates since the start date of the hindcast, a lengthening of the ensemble time series with the 45 days of ERA-40 data previous to the hindcast start date was required. However, this also implies that the analysis corresponding to the initial 45 days of the simulations contains some influence from ERA-40. Figure 8 shows the ratio of the variance of the local modes to the corresponding total filtered variance averaged for the analysis carried out for the period from 45 to 135 days of hindcast (i.e., there is no influence from the appended ERA-40 data) for all members and hindcasts. The reference in this case is the NOAA OLR dataset5. The simulated local modes retain much less variance than the reference, which can be interpreted as a lack of organization of the convection in the hindcasts. This bias is more obvious in the case of ECMWF and UKMO, in agreement with previous results. Therefore, not only the filtered variability for these two models is underestimated, but it is also less spatially coherent than in the reference.

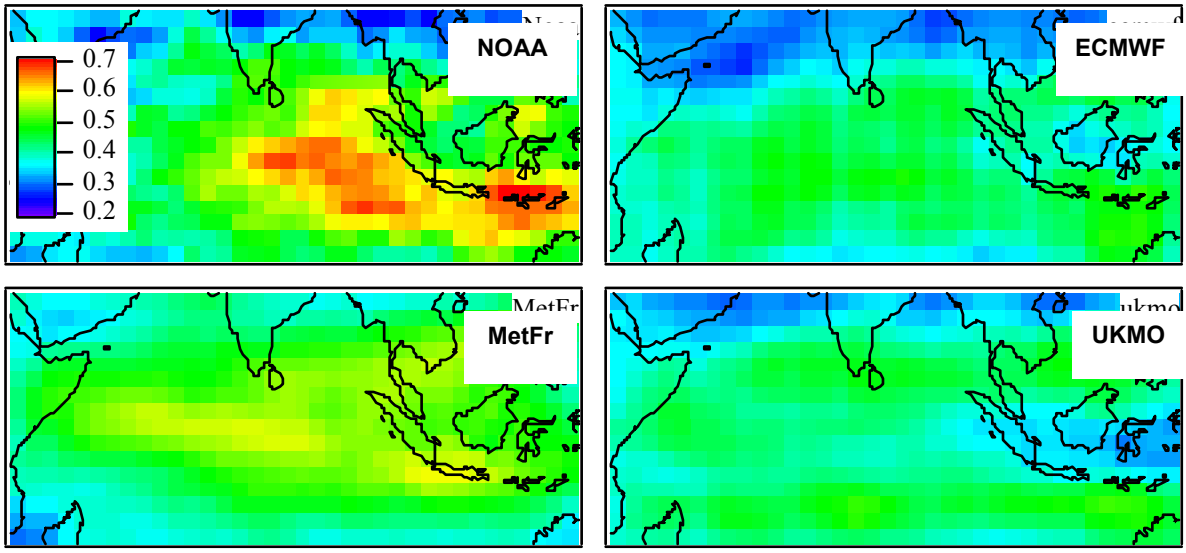

Figure 8: Ratio of the variance retained by the local modes to the filtered variance for each 90-day window from 45 days after the start of the hindcast until 45 days before the end for every winter OLR ensemble hindcast over the period 1980-2001. The local mode analysis has been performed on 90-day moving window time series with an interval between consecutive windows of 5 days. The results have been averaged for all members and hindcasts. The reference is the NOAA OLR dataset.

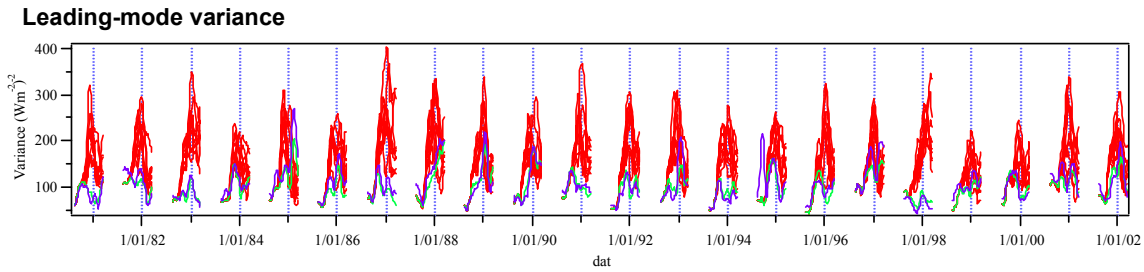

Figure 9: Variance of the leading mode of boreal winter OLR for each 90-day window from the start of the hindcast until 45 days before the end over the period 1980-2001. The results for the MetFr ensemble hindcasts are displayed in red, while the variances for the NOAA and ERA-40 datasets appear in purple and green, respectively. The local mode analysis has been performed on 90-day moving window time series with an interval between consecutive windows of 5 days.

[5] Data available from http://www.cdc.noaa.gov/cdc/data.interp_OLR.html

The set of leading modes can be considered as an estimate of the activity of the intra-seasonal variability within the window used for the analysis. In particular, an ensemble of leading modes for a specific time is available from each ensemble hindcast. As an example, Figure 9 shows the variance of the leading mode for each 90-day window from 45 days before the start of the hindcast until 45 days before the end for every winter hindcast of the period 1980-2001. The results for the MetFr ensemble are displayed in red, while the variances for the NOAA and ERA-40 datasets appear in purple and green, respectively. The differences between these two datasets are small (the interannual correlation between the leading mode variances identified in both datasets is close to 0.9), OLR variance being larger for NOAA than for ERA-40. The filtered variance is overestimated for every single hindcast, the spread being as large as the interannual variations (not shown). The leading-mode variance is also overestimated, although the relative difference with the reference is reduced when compared to the case of the filtered variance. This is in agreement with the smaller coherent space-time organization of the variability in the model shown in Figure 8 for the local modes. However, Figure 10a indicates that the percentage of variance for this particular model is close to that of the reference. Therefore, although the intra-seasonal variance is overestimated for nearly all grid points, the intra-seasonal variability of the convection is not as well organised at large scale as in the reference (lower variance percentage), the spatial pattern of the modes being more variable and the geographical distribution of the percentage of explained variance having more spread.

The ensemble leading modes show an excessive spread of the leading-mode variance, although in some cases it allows to capture the verification within the ensemble. The spread should also be understood as the existence of very different local modes (i.e., different spatial patterns, thus large variability of amplitude and phase of the oscillations) for different ensemble members of the same hindcast (not shown). In addition, the interannual variability does not seem to be well reproduced. For instance, the warm ENSO years 1983 and 1998 show a small variance for the reference, while the coupled model seems to display more activity than normal. The interannual correlation between the variance in the hindcasts and the reference is shown in Figure 10b. This correlation decreases steadily since the time when the first hindcast data are used (first vertical bar) and by the time there is no influence of the appended ERA-40 data (third vertical bar) it becomes close to zero. This apparent lack of predictability requires further research using the local modes as well as the leading modes, with additional analyses carried out for other regions, such as the western Pacific, as well as for other seasons.

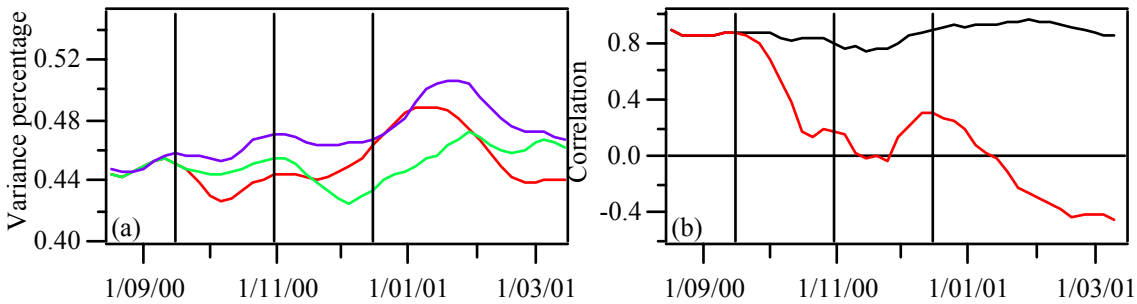

Figure 10: (a) Average ratio of variance of the leading mode to the filtered variance for each 90-day window from 90 days before the start of the hindcast for every winter OLR ensemble hindcast over the period 1980-2001. The results for the MetFr ensemble hindcasts are displayed in red, while the variances for the NOAA and ERA-40 datasets appear in purple and green, respectively. (b) Interannual correlation between the leading-mode variance of the reference and simulated datasets for each pendad (red) and between the two reference datasets (black). The local mode analysis has been performed on 90-day moving window time series with an interval between consecutive windows of 5 days and the results averaged for all members and hindcasts. The vertical bars inside each plot represent, from left to right, the time when hindcast data start to be included in the 90-day analysis window, the start date of the hindcast and the time when no ERA-40 data have been appended to the 90-day analysis window.

6. Summary and discussion

The DEMETER multi-model dataset has been analyzed using a variety of techniques such as time filtering, wavenumber-frequency spectral analysis and EOF analysis to identify the characteristics of tropical intra-seasonal oscillations. The models display a wide range of skill in simulating the intra-seasonal variability. Although a clear seasonal signal in the variance of wind, temperature and OLR with greatest activity during boreal winter is observed, most models, except for those using the ARPEGE atmospheric GCM, underestimate the strength of the intra-seasonal variability and misrepresent its geographical distribution. The wavenumber-frequency spectral analysis has shown that the spectral properties of the oscillations are different when analysing different variables, such as OLR and winds. In addition, it indicates that the under or overestimation of the intra-seasonal variability may be due to drawbacks in the representation of particular oscillations, such as the Kelvin waves or the MJO. In the particular case of the MJO, some models show evidence of an eastward propagating anomaly in the wind and temperature fields, with most models showing a tendency for a standing oscillation in the OLR. Where a model has a clear eastward propagating signal, typical periodicities seem quite reasonable. Otherwise, the typical periods appear to be too long. The EOF analysis has been carried out to detect the large-scale characteristics of the fields. Among the models discussed here, MetFr seems to simulate large-scale intra-seasonal oscillations with the most realistic features. Therefore, given that the structure of the large-scale perturbations, in particular the MJO, should be understood in terms of scale interaction between large-scale circulations and mesoscale systems, a correct representation of the whole spectrum is required. As a consequence, a comprehensive diagnostic of the tropical intra-seasonal variability covering a wide range of periods and scales should be undertaken to document the phenomena involved.

Errors in intra-seasonal variability seem mainly dependent on the atmospheric component of the coupled model. Nevertheless, ocean-atmosphere coupling plays a relevant role in the correct simulation of the intra-seasonal oscillations, although the specific choice of the ocean component appears to be of secondary importance. This indicates that similar benefits may be attained when using a simplified ocean model.

The local mode analysis method has been illustrated as both an efficient way to detect modes of variability of intermittent phenomena and to estimate the predictability of the activity of the intra-seasonal variability. A weaker spatial coherence of the large-scale signals, estimated as the variance explained by the leading mode, has been found in the models when compared to a reference dataset. This agrees with the errors observed in the wavenumber-frequency spectral analysis. The models tend to present a set of leading local modes with a large range of percentage of variance for the different ensemble members of a hindcast. This can be interpreted as the hindcasts having an excessive spread, which is larger than the interannual variability of the activity. In addition, no obvious signs of interannual predictability have been found, although more detailed research is being carried out.

In general terms, the relationship between a model's intra-seasonal activity, its seasonal cycle and the characteristics of its basic climate represents relevant information for the understanding of the model predictive behaviour. In addition, it becomes evident that an accurate description of the basic climate in terms of mean state and variability may be a prerequisite for improving the simulation of realistic intra-seasonal oscillations and their interactions with the modes of variability responsible for the predictability at the seasonal time scale.

7. Acknowledgements

The DEMETER project has been funded by the European Union under the contract EVK2-1999-00197.

8. References

Goulet, L. and J.-P. Duvel (2000). A new approach to detect and charcterize intermittent atmospheric oscillations: Application to the intraseasonal oscillation. *J. Atmos. Sci.*, **57**, 2397-2416.

Innes, P. and J. M. Slingo (2003). Simulation of the Madden-Julian Oscillation in a coupled general circulation model. Part I: Comparison with observations and an atmosphere-only GCM. *J. Climate*, **16**, 345-364.

Palmer, T. N., Ĉ. Brankovic and D. S. Richardson (2000). A probability and decision-model analysis of PROVOST seasonal multi-model ensemble integrations. *Quart. J. Roy. Meteor.Soc.*, **126**, 2013-2034.

Palmer, T. N., A. Alessandri, U. Andersen, P. Cantelaube, M. Davey, P. Délécluse, M. Déqué, E. Díez, F. J. Doblas-Reyes, H. Feddersen, R. Graham, S. Gualdi, J.-F. Guérémy, R. Hagedorn, M. Hoshen, N. Keenlyside, M. Latif, A. Lazar, E. Maisonnave, V. Marletto, A. P. Morse, B. Orfila, P. Rogel, J.-M. Terres, M. C. Thomson (2004). Development of a European multi-model ensemble system for seasonal to inter-annual prediction (DEMETER), *Bull. Amer. Meteor. Soc*., in press.

Slingo, J. M., D. P. Rowell, K. R. Sperber and F. Nortley (1999). On the predictability of the interannual behaviour of the Madden-Julian Oscillation and its relationship with El Niño. *Quart. J. Roy. Meteor.Soc.*, **125**, 583-609.

Slingo, J. M., K. R. Sperber, J. S. Boyle, J-P. Ceron, M. Dix, B. Dugas, W. Ebisuzaki, J. Fyfe, D. Gregory, J-F. Gueremy, J. Hack, A. Harzallah, P. Inness, A. Kitoh, K-M. Lau, B. McAvaney, R. Madden, A. Matthews, T. N. Palmer, C-K. Park, D. Randall and N. Renno (1996). Intraseasonal oscillations in 15 atmospheric general circulation models: Results from an AMIP diagnostic subproject. *Climate Dyn.*, **12**, 325-357.

Stockdale, T. N., D. L. T. Anderson, J. O. S. Alves and M. A. Balmaseda (1998). Global seasonal rainfall forecasts using a coupled ocean-atmosphere model. *Nature*, **392**, 370-373.

von Storch, H. and F. W. Zwiers (1999). *Statistical Analisis in Climate Research*. Cambridge Univ. Press, 484 pp.

Wheeler, M. and G. N. Kiladis (1999). Convectively coupled equatorial waves: Analysis of clouds and temperature in the wavenumber-frequency domain. *J. Atmos. Sci.*, **56**, 374-399.